This is a preprint, the final version is subject to change, of the American Mineralogist (MSA)
Cite as Authors (Year) Title. American Mineralogist, in press.
(DOI will not work until issue is live.) DOI: http://dx.doi.org/10.2138/am-2017-5953

Revision 1

Field-based accounting of CO_2 sequestration in ultramafic mine wastes using portable X-ray diffraction

Connor C. Turvey[1]*, Siobhan A. Wilson[1], Jessica L. Hamilton[1], Gordon Southam[2]

[1]School of Earth, Atmosphere & Environment, Monash University, Clayton, Melbourne, Victoria 3800, Australia

[2]School of Earth Sciences, The University of Queensland, St Lucia, Queensland 4072, Australia

* Corresponding author, connor.turvey@monash.edu, +61 03 9905 4382

This is a preprint, the final version is subject to change, of the American Mineralogist (MSA)
Cite as Authors (Year) Title. American Mineralogist, in press.
(DOI will not work until issue is live.) DOI: http://dx.doi.org/10.2138/am-2017-5953

Abstract

Carbon mineralisation, the sequestration of carbon within minerals, presents one method through which we could control rising levels of anthropogenic carbon dioxide (CO_2) emissions. The mineral wastes produced by some ultramafic-hosted mines have the ability to sequester atmospheric CO_2 via passive carbonation reactions. Carbon accounting in mine tailings is typically performed using laboratory-based quantitative X-ray diffraction (XRD) or thermogravimetric methods, which are used to measure the abundances of carbonate-bearing minerals such as hydromagnesite [$Mg_5(CO_3)_4(OH)_2 \cdot 4H_2O$] and pyroaurite [$Mg_6Fe^{3+}_2(CO_3)(OH)_{16} \cdot 4H_2O$]. The recent development of portable XRD instruments now allows for the characterisation and quantification of minerals in the field. Here we assess the feasibility of using a portable XRD instrument for field-based carbon accounting in tailings from the Woodsreef Chrysotile Mine, New South Wales, Australia. Modal mineralogy was obtained by Rietveld refinements of data collected with an inXitu Terra portable XRD. The Partial Or No Known Crystal Structures (PONKCS) method was used to account for turbostratic stacking disorder in serpentine minerals, which are the dominant phases in tailings from Woodsreef. Weighed mixtures of synthetic tailings were made to evaluate the precision and accuracy of quantitative phase analysis using the portable instrument. An average absolute deviation (bias) of 8.2 wt% from the actual composition of the synthetic tailings was found using the portable instrument. This is comparable to the bias obtained using a laboratory-based diffractometer (9.6 wt% absolute) and to the results from previous quantitative XRD studies involving serpentine minerals. The methodology developed using the synthetic tailings was then applied to natural tailings samples from Woodsreef. Surface crusts forming on the tailings pile were found to contain hydromagnesite (~5.8 wt%) and pyroaurite (~2.1 wt%). Comparable results were

obtained using the laboratory-based instrument and these results are expected to have similar biases to the analyses of the synthetic tailings. These findings demonstrate that portable XRD instruments may be used for field-based measurement of carbon sequestration in minerals in engineered and natural environments.

Keywords: carbon accounting, carbon sequestration, carbon mineralisation, portable X-ray diffraction, PONKCS method, Rietveld refinement, chrysotile, hydromagnesite, pyroaurite.

Introduction

Carbon dioxide (CO_2) sequestration strategies seek to mitigate the adverse impacts of anthropogenic climate change by preventing release of this greenhouse gas to the atmosphere or by capturing it directly from the air (IPCC, 2013; IPCC, 2014). Carbon mineralisation is one approach to CO_2 sequestration whereby CO_2 is trapped and stored within the crystal structures of carbonate minerals over geologic timescales (Kump et al., 2000; Lackner, 2003; Lackner et al., 1995; Matter et al., 2016; Seifritz, 1990). These carbonate minerals are formed through the reaction of aqueous carbonate anions with divalent metal cations, typically Mg^{2+} and Ca^{2+}, which are released during weathering of silicate and hydroxide minerals. Such weathering reactions occur naturally where Mg- and Ca-rich mafic and ultramafic rocks, are exposed to the atmosphere (Lackner, 2002; Oelkers et al., 2008; Power et al., 2013).

Engineered landscapes such as the tailings storage facilities associated with ultramafic-hosted mines provide a suitable location for rapid carbon mineralisation (Wilson et al., 2006). This is because mineral processing drastically reduces grain size and increases the surface area available for carbonation reactions within the tailings (Wilson et al., 2009a). Previous studies have detailed the carbonation of ultramafic mineral wastes at mines in Canada, Australia and Norway. These

include the Diavik Diamond Mine (Wilson et al., 2009b), Clinton Creek Chrysotile Mine (McCutcheon et al., 2015; Wilson et al., 2009a), Cassiar Chrysotile Mine (Wilson et al., 2009a), Turnagain Nickel Project (Hitch et al., 2010), and Black Lake Mine in Canada (Assima et al., 2012; Lechat et al., 2016; Pronost et al., 2012). Localities outside of Canada include mine sites within the Feragen ultramafic body in Norway (Beinlich and Austrheim, 2012) as well as the Mount Keith Nickel Mine (Bea et al., 2012; Harrison et al., 2013; Wilson et al., 2014) and Woodsreef Chrysotile Mine, in Australia (McCutcheon et al., 2016; Oskierski et al., 2013a; Oskierski et al., 2013b).

The Woodsreef chrysotile deposit is located in New South Wales and was the site of the only large-tonnage chrysotile mine in Australia. During its lifetime the Woodsreef chrysotile mine produced 550,000 t of long fibre chrysotile, 24 Mt of tailings and 75 Mt of waste rock (Laughton and Green, 2002; Merril et al., 1980). A previous study of carbon mineralisation at Woodsreef determined sequestration of atmospheric CO_2 was occurring within thin crusts of hydromagnesite [$Mg_5(CO_3)_4(OH)_2 \cdot 4H_2O$] and sedimentary pyroaurite [$Mg_6Fe^{3+}_2(CO_3)(OH)_{16} \cdot 4H_2O$] that have formed at or near the surface of the tailings pile (Oskierski et al., 2013b). Oskierski et al. (2013b) estimated that between 1400 and 70,000 t of atmospheric CO_2 has been sequestered at Woodsreef since the closure of the mine in 1984. As a derelict mine site, Woodsreef presents an excellent location to conduct studies into how to maximise the carbonation rate of ultramafic tailings through biotic and abiotic processes (McCutcheon et al., 2016). Strategies found to enhance the carbonation of tailings at derelict mines such as Woodsreef could be applied at operating mines, with the ultimate goal of creating carbon neutral mining practices (Power et al., 2014; Wilson et al., 2014).

Determining the carbon sequestration potential of mine tailings is typically performed using laboratory-based quantitative X-ray diffraction (XRD) or thermogravimetric methods, which are used to measure the abundances of carbonate-bearing minerals derived from weathering reactions. Studies typically include an extensive sampling regime across a large area to account for mineralogical variability in a tailings facility (Wilson et al., 2009a; Wilson et al., 2014; Wilson et al., 2009b). Portable XRD instruments allow for the possibility of detecting and quantifying CO_2 storage in minerals while in the field, enabling just-in-time modification of a sampling strategy. This would allow the most important and representative samples to be taken. Although portable XRD is not necessarily a replacement for laboratory-based sample analysis, it could be used to prevent sampling bias and knowledge gaps that must be rectified with subsequent excursions and sampling. In this way, portable XRD instruments constitute an untapped asset when conducting carbon accounting in minerals on the landscape scale, especially when investigating a field site for the first time.

The proliferation of field-portable XRD instruments began following the development of the CheMin instrument as part of the Mars Science Laboratory (MSL) mission (Bish et al., 2013; Vaniman et al., 1998). Clay bearing samples collected by the MSL Curiosity rover at Gale Crater on Mars have been analysed very successfully using the FULLPAT methodology (Chipera and Bish, 2002). However portable XRD instruments have not previously been used for carbon accounting and it is unknown whether they can be employed to accurately quantify mineral abundances in serpentine rich ultramafic rocks and mine tailings. Quantifying the mineralogical composition of ultramafic rocks and mineral wastes that contain serpentine minerals is challenging using XRD data and traditional Rietveld refinement approaches. This is because

serpentine minerals suffer from turbostratic stacking disorder, which produces broad anisotropic diffraction peaks that are difficult to model.

Several Rietveld compatible approaches have been developed to overcome this difficulty and permit quantification of structurally disordered clay phases such as serpentine minerals (Chipera and Bish, 2002; Scarlett and Madsen, 2006; Taut et al., 1998; Wilson et al., 2006). For high throughput, field-based quantification of clay minerals (such as serpentines) at mine sites, the method of Scarlett & Madsen (2006) is likely to be the most suitable approach. This is because it can be used to quantify phases with partially known or no known crystal structures (PONKCS) (Scarlett and Madsen, 2006), and once calibrated, this method does not require (1) addition of an internal standard to samples, (2) specialised and labour-intensive preparation of specimens, or (3) experimental reference patterns for all constituent minerals in a sample.

Here, we use a series of synthetic, carbonate-bearing chrysotile mine tailings samples with known compositions to test the accuracy of quantitative phase analysis using the PONKCS methods (Scarlett and Madsen, 2006) and portable XRD data. Rietveld refinement results of diffraction patterns collected with an inXitu Terra portable XRD are compared with those obtained from refinement of patterns collected with a laboratory-based Bruker D8 Advance diffractometer. This analytical approach is then applied to estimate the amount of CO_2 sequestered in representative samples of carbonated tailings from the Woodsreef Chrysotile Mine. We found that modal mineralogy obtained using a portable XRD instrument can be of comparable accuracy to that obtained using a laboratory instrument. Thus, portable XRD may be used for field-based crystallographic accounting of CO_2 sequestration at Woodsreef and other ultramafic mines. Furthermore, the use of portable XRD could be extended to other mineralogically complex, clay-bearing systems, such as soils and sediments.

This is a preprint, the final version is subject to change, of the American Mineralogist (MSA)
Cite as Authors (Year) Title. American Mineralogist, in press.
(DOI will not work until issue is live.) DOI: http://dx.doi.org/10.2138/am-2017-5953

132 # Experimental Section

133 ## Field sampling methods

134 Samples were taken from the tailings pile at the Woodsreef Chrysotile Mine, New South Wales,
135 Australia in late April and early May 2013. These include several carbonated surface crusts, a
136 sample of shallow unconsolidated tailings and a partially carbonated vein of chrysotile found
137 within a large cobble of waste rock (Figure 1). These samples were collected to assess the extent
138 of carbonation that has occurred following milling and deposition of tailings and to investigate
139 variation in the mineralogy of waste rock, unconsolidated tailings material and surface crusts.
140 Samples were chosen to provide an overview of the geochemical processes occurring at
141 Woodsreef such that the results of this study could then be used to plan for a more extensive
142 sampling regime in the future.

143 Insert Figure 1 hereabouts

144 ## Sample Preparation and Data Collection

145 Four artificial tailings samples of known composition were prepared to evaluate the accuracy of
146 Rietveld refinement results obtained using the PONKCS method and portable XRD data. The
147 artificial samples were used to test multiple refinement strategies, similar to the methodology
148 used by Wilson et al. (2006). Rietveld refinement results were compared to known mineralogical
149 compositions (Table 1) of the artificial tailings samples. Refinement methods that produced the
150 least relative and absolute error on estimates of mineral abundance for the artificial samples were
151 then applied to tailings samples from Woodsreef.

152 The artificial tailings samples were made to reflect the mineralogy of Woodsreef tailings
153 according to qualitative XRD results (Figure 2) and the work of Oskierski et al. (2013b).

Serpentine group minerals [$Mg_3Si_2O_5(OH)_4$] were the most abundant phases observed and magnetite, hydromagnesite and pyroaurite, a carbonate-bearing hydrotalcite group mineral, were present as minor phases. The composition of each artificial tailings sample was varied to cover a range of abundances for each minor phase (Table 1). Selected compositions were chosen based on the work of Oskierski et al. (2013) who found that abundances of hydromagnesite were typically <15 wt% and that pyroaurite abundance was typically ~5 wt% (see Supplementary Information for descriptions of the minerals used to make the synthetic tailings samples).

Insert Table 1 hereabouts.

Insert Figure 2 hereabouts.

All synthetic and natural tailings samples were analysed using both an inXitu Terra portable diffractometer located in the School of Earth, Atmosphere and Environment at Monash University and a Bruker D8 Advance diffractometer located in the Monash X-ray Platform. The same subsample was used for data acquisition on both instruments to ensure that any discrepancies in Rietveld refinement results would be due solely to instrumental differences, rather than differences in particle size or heterogeneities in mineral abundances. The natural tailings samples collected from Woodsreef were pulverised using a ring mill and both natural and artificial samples were then milled for 7 minutes under ethanol using a McCrone Micronizing Mill. Samples analysed using the Bruker D8 were placed in back loading cavity mounts and loaded against frosted glass to reduce the effects of preferred orientation.

Samples analysed used the D8 were analysed for 65 minutes. A range of analysis times were trialled using the inXitu Terra, ranging from 15 minutes to 128 minutes. An analysis time of 128 minutes was used to ensure the resolution of minor phases at or near the instruments detection

limit (see Results section for differences in analysis times). Mineral identification was performed using DIFFRAC.EVA V.2 (available from Bruker AXS) with reference to, standard patterns from the ICDD PDF-2 database and the Crystallography Open Database (see Supplementary Information for instrument details and analytical conditions used to collect XRD patterns).

Rietveld refinement strategy

Quantitative phase analysis was performed using a modified version of the Rietveld method (Bish and Howard, 1988; Hill and Howard, 1987; Rietveld, 1969) for phases with Partial Or No Known Crystal Structures (PONKCS) (Scarlett and Madsen, 2006). The Rietveld method uses a calibration factor for the quantification of each phase, derived from the mass and volume of its unit cell. Typically, this means that a Rietveld refinement requires that all phases within a given sample be highly crystalline and have well known crystal structures (Bish and Howard, 1988). The serpentine polymorphs found in Woodsreef tailings (i.e., chrysotile and lizardite) have disordered crystal structures that are characterised by turbostratic stacking disorder. This results in severe anisotropic peak broadening in powder XRD patterns. Such peak profiles cannot be modelled using a traditional Rietveld refinement approach that relies upon the availability of structural information derived from well-crystallised mineral specimens. Previous studies focussing on carbon accounting in serpentine-rich samples have successfully overcome this challenge through the use of a Pawley phase (Pawley, 1981) for structureless pattern fitting and the introduction of an internal standard (Wilson et al., 2014; Wilson et al., 2006; Wilson et al., 2009b). This approach treats the disordered phase as though it were amorphous for the purposes of quantification.

The PONKCS method (Scarlett and Madsen, 2006) allows for the quantification of disordered phases without the addition of an internal standard in every sample, making it more flexible and

199 better adapted to quantitative phase analysis for portable XRD data in the field. This is a method
200 whereby the peaks of a PONKCS phase are modelled using structureless profile fitting and its
201 Rietveld refinement parameters, *Z*, *M* and *V*, are calibrated against those of a highly crystalline
202 and well-characterised phase. The relative peak intensities and Rietveld refinement parameters,
203 which lack physical meaning with reference to the crystal structure of the mineral in question,
204 are then fixed and may be used for phase quantification of polymineralic samples (Scarlett and
205 Madsen, 2006).

206 Two standard samples were made for calibration of PONKCS models consisting of a 50:50 wt%
207 mixture of: (1) chrysotile sourced from Clinton Creek, Yukon, Canada and NIST 676a α-Al_2O_3
208 and (2) lizardite sourced from The University of British Columbia and NIST676a α-Al_2O_3. A
209 calibrated mass, *M*, value for the unit cell of each phase was obtained by Rietveld refinement of
210 the binary mixtures in the program Topas v.3 (Bruker AXS). Chrysotile and lizardite peaks were
211 fit using the Pawley method of structureless pattern fitting (Pawley, 1981). Unit cell parameters
212 and space groups were derived from previous studies: Falini et al. (2004) for chrysotile and
213 Mellini and Viti (1994) for lizardite. These parameters were used to obtain the *Z* and *V*
214 refinement parameters for chrysotile and lizardite. A spherical harmonics correction (Järvinen,
215 1993) was used to model anisotropic peak shape in both serpentine phases; the model parameters
216 were allowed to vary during refinement following the method of Wilson et al. (2006, 2009). The
217 resulting calibrated PONKCS models for chrysotile and lizardite can be used in a similar manner
218 as crystal structure information when performing Rietveld refinements (Scarlett and Madsen,
219 2006).

220 Once the PONKCS models for chrysotile and lizardite had been generated, they were introduced
221 as appropriate into refinement models for all samples including the artificial tailings samples and

Woodsreef tailings samples. Rietveld refinements were carried out with the program Topas v.5 (Bruker AXS) using the fundamental parameters approach (Cheary and Coelho, 1992). Background functions were modelled using second-order Chebychev polynomials with an additional $1/x$ function. A default Brindley radius of 0.00025 mm and a packing density of 0.4 were used to correct for microabsorption contrast amongst all phases (Brindley, 1945).

Multiple variations of the Rietveld refinement approach were performed upon the data for the artificial tailings samples and the results were compared to the known compositions. The results were used to determine the best refinement methodology for natural tailings samples from Woodsreef. Two different refinement strategies were adopted, one for each of the XRD instruments (see Supplementary Information for details).

Results

Analysis time comparison for the inXitu Terra

The analysis time for the inXitu Terra was varied for a single sample (Artrock1, see Table 1 for weighed composition) to determine how great an impact analysis time had upon the quality of data produced by the instrument. Multiple analyses were performed upon the sample, with analysis times ranging from 15 to 128 minutes (Figure 3). This was done with the aim of determining how many exposures were required to reliably discern the peaks of minor phases above the background radiation signal. This analysis allowed for identification of the shortest analysis time that could result in the reliable identification of minor phases. Rapid analysis could be a great asset when conducting XRD analysis in the field, allowing for rapid identification and quantification of minerals.

Insert Figure 3 Here.

Figure 3 compares XRD patterns collected from Artrock1 with the inXitu Terra using acquisition times of 15, 60 and 128 minutes. The characteristic peaks of chrysotile (89.0 wt%) and magnetite (7.0 wt%) are readily identifiable in all of the patterns; however, the peaks for pyroaurite and hydromagnesite (both of which are present at between 1−2 wt% abundance) are harder to reliably discern above the background. The difficulty of identifying these minerals implies their abundances are near the detection limit of the instrument, and that this limit is between 1−2 wt% abundance. This mirrors the findings of Bish et al. (2013) who performed quantitative analysis of samples on Mars using the CheMin instrument aboard the Mars Science Laboratory rover, Curiosity (the instrument on which the inXitu Terra design is based) (Blake et al., 2013). Bish et al. (2013) report a comparable detection limit of below 3 wt% abundance. Although detection of these minor phases is problematic it is enhanced with increasing acquisition time, which improves the signal to noise ratio. For the shortest analysis time (15 minutes) the diagnostic hydromagnesite peak at 18° 2θ cannot be reliably detected over the background signal. However, in the 60-minute analysis this peak can be more clearly identified. Similarly, the pyroaurite peak at 13° 2θ is difficult to discern even in the 60 minute run time owing largely to overlap with the basal peak of chrysotile. The 128-minute acquisition does allow detection of this peak (although it could still be missed as a consequence of overlap with chrysotile).

This means that a relatively long analysis time is required for the inXitu Terra if all minor phases need to be reliably identified and/or quantified. As such, for our study an analysis time of 128 minutes was chosen to facilitate the production of high quality data for the inXitu Terra, thus allowing a better comparison to the laboratory based instrument. However, there are circumstances, when faster acquisition of lower resolution patterns might be required, particularly when conducting analyses in the field. If minor phases were present in higher

abundances (i.e., greater than the 1−2 wt% detection limit) then a faster run time could be employed. As such, faster acquisition times could be used if only qualitative analysis and detection of mineral phases were is required. In such cases a shorter run time of 30−60 minutes would likely be appropriate.

Artificial tailings samples

Refined modal abundances for the four artificial tailings samples are compared with known values in Table 1. The sum of the absolute deviations from the actual composition (total bias) is reported for each refinement result. The total bias value was developed by Omotoso et al. (2006) to compare the results produced by different quantitative X-ray diffraction strategies when working with samples of known mineralogical compositions (Omotoso et al., 2006). Rietveld refinement results for inXitu Terra data using the PONKCS method have an average total bias of 8.2 wt% across the four synthetic samples (average bias per phase of 1.6 wt%). Results for Bruker D8 Advance patterns have an average total bias of 9.6 wt% across the four synthetic samples (average bias per phase of 1.9 wt%). Figure 4 plots the absolute and relative errors between refined and known abundances of each phase in the artificial tailings samples.

Insert Figure 4 hereabouts

Refined values for chrysotile abundances, using data obtained with both the portable and laboratory instruments, have the highest absolute errors of any phases with values between 1.1 and 6.1 wt%. However, because chrysotile is present at significantly higher abundances than any other phase in the artificial tailings samples (>70 wt%), it has the lowest relative error values of any phase (1.2−7.7 %). The refined abundance of hydromagnesite was consistently underestimated wherever present at higher abundances (i.e., >5 wt%). Absolute errors on

289 estimates of hydromagnesite abundance vary between 0.3 and 3.9 wt% for samples with known
290 hydromagnesite abundances of 5 wt% or higher. Refined values for magnetite abundance are
291 within 2.7 wt% absolute of the known values (5.0−7.1 wt% magnetite). Magnetite abundances
292 are consistently over estimated by the inXitu Terra data (from +0.2 to +2.2 wt% of the actual
293 values). Magnetite abundances refined from patterns generated by the Bruker D8 Advance are
294 consistently underestimated (from −1.5 to −2.7 wt% of the actual values).

295 The least abundant phases across all samples, brucite and pyroaurite, were typically
296 underestimated using data obtained with both instruments, with errors of between -0.2 and -2.1
297 wt%. In only one case was the abundance of one of these phases overestimated: the reported
298 abundance of brucite in sample Artock1 (known to be 1.0 wt%) was refined to a value of 2.2 wt%
299 when using data collected with the Bruker D8 (an error of +1.2 wt%). Relative errors are
300 inversely proportional to mineral abundance with minor phases having the highest relative error
301 values, a trend that has been found in similar quantitative XRD studies (Wilson et al., 2006;
302 Wilson et al., 2009b). In two cases, these error values were 100% relative or greater. The trend of
303 high absolute errors occurring for high abundance phases is advantageous as even the highest
304 absolute error value of 6.1 wt% yields a small relative error of 7.7% (i.e., for chrysotile
305 abundance in sample Artrock3 using data from the Bruker D8).

306 There is little difference in the average bias values for refinement results across the two XRD
307 instruments. Refinement of data obtained using the Bruker D8 Advance, produced an average
308 total bias across the four synthetic samples of 9.6 wt% and typical relative errors of 40% or less
309 for phases present at abundances <10 wt% (Figure 4c). The most significant difference observed
310 is that refinement of inXitu Terra data yields considerably higher relative error values for phases
311 present at very low abundances. Relative error values of 80% or less are typical for phases

present at <3.5 wt% (Figure 4d); however, for minor phases present at >3.5 wt% abundance, relative error is typically <40%, comparable to refinement results obtained using Bruker D8 Advance data. The average total bias value obtained from refinement of inXitu Terra data is comparable to, and slightly lower than, that for the Bruker D8 Advance at 8.2 wt%. These results are encouraging for performing quantitative XRD in the field, with the only major advantage of using a laboratory-based XRD being improved detection limits and more accurate abundances for trace phases. Furthermore, these error levels are comparable to the error margins reported from other studies using similar methods (Wilson et al., 2006). Nonetheless, it is important to note that these results are for analysis of micronized samples using a field-portable instrument and a laboratory-based instrument. Further assessment will need to be done on samples with a coarser grain size to be directly applicable to quantitative phase analysis of samples in the field.

Woodsreef tailings samples

Once analysis of the artificial tailings samples was completed the natural tailings samples from Woodsreef were analysed using both the inXitu Terra and the Bruker D8 diffractometer. The mineralogy of the naturally occurring samples from the Woodsreef mine is broadly consistent across the tailings pile with the most prominent major phases being the serpentine minerals, lizardite and chrysotile. The most common minor phases are magnetite and pyroaurite. The most noticeable change in mineralogy across the six Woodsreef tailings samples is found in the surface crusts. Here, hydromagnesite appears to be more abundant and its precipitation acts to cement tailings grains into a coherent mass (Figure 1 and 2). Trace phases, present at abundances near the detection limit of the inXitu Terra, include quartz, hematite and forsterite. These results are consistent with the findings of Oskierski et al. (2013b) who report modal mineralogy of Woodsreef tailings as part of a study using a laboratory-based diffractometer.

335 The same Rietveld refinement approach used for synthetic tailings was applied to patterns from
336 the six samples of tailings collected from Woodsreef. Table 2 summarizes refinement results for
337 data obtained from both the Bruker D8 Advance and inXitu Terra. Serpentine (likely a mix of
338 lizardite and chrysotile) dominates, comprising >72 wt% of all samples. Sample 13WR2-6
339 consists of shallow unconsolidated tailings taken from the top 30 cm of the tailings pile. It
340 contains the highest abundance of serpentine minerals: 93.2 wt% according to the inXitu Terra
341 refinement and 82.7 wt% according to the Bruker D8 refinement. The surface crusts contain
342 hydromagnesite as the most prominent of the minor phases with abundances of between 2.2−8.8
343 wt% (using inXitu Terra data) or 6.7−12.5 wt% (using Bruker D8 Advance data). Magnetite and
344 pyroaurite were found in all six samples. Sample 13WR1-3, a partially carbonated chrysotile
345 vein found within a hand sample of waste rock, had a similar mineralogy to the surface crusts
346 with a hydromagnesite abundance of 5.3 wt% (inXitu Terra) and 4.9 wt% (Bruker D8 Advance).
347 Sample 13WR1-3 also contained the highest reported abundance of pyroaurite of all the samples
348 analysed, 13.6 wt% according to refinement of data from the Bruker D8 Advance. This
349 pyroaurite abundance appears to be anomalously high, with refinement of the inXitu Terra data
350 giving a value of 2.9 wt% for the same sample.

351 Insert Table 2 hereabouts

352 The large degree of variation between the results obtained from the two instruments for sample
353 13WR1-3 is representative of a larger trend observed for analysis of Woodsreef samples. There
354 is a larger degree of variation for the reported mineral abundances between instruments for the
355 natural samples than in the artificial samples. This variation could be attributed to the presence of
356 more trace phases in the natural Woodsreef samples than in the synthetic tailings. Refinements of
357 inXitu Terra data appear to be overestimating the abundance of serpentine minerals at the

358 expense of the minor minerals in samples that contain large numbers of phases. The lower
359 abundances of pyroaurite in refinements of inXitu Terra data can be attributed to the way the
360 instrument vibrates a sample in the sample cell to reduce preferred orientation. This method may
361 be more successful at reducing preferred orientation than the combination of back loading
362 against frosted glass and applying the March-Dollase preferred orientation correction (Dollase,
363 1986; March, 1932) that is used for acquisition of Bruker D8 Advance data.

364 Refinements for the natural Woodsreef tailings included more minor and trace phases than the
365 artificial tailings samples. The Bruker D8 Advance has a superior detection limit to the inXitu
366 Terra, producing XRD patterns that typically reveal more trace phases for a given sample.
367 Including these trace phases in refinements using the Bruker D8 leads to lower refined serpentine
368 abundances. The variation between phase abundances could also be attributed to the size of the
369 sample analysed by each instrument. The back loading cavity mounts used for analysis of
370 samples with the Bruker D8 Advance contain a larger volume of sample than can be
371 accommodated by the sample chamber in the inXitu Terra. It is possible, but unlikely for
372 micronised samples, that the inXitu Terra is more susceptible to analysis of smaller, less
373 representative subsamples of tailings. Because refinements using inXitu Terra data tend to
374 provide lower estimates of the abundances of hydromagnesite and pyroaurite, the quantitative
375 assessment of carbon sequestration in ultramafic mine tailings using the inXitu Terra will mostly
376 likely represent a lower bound and a conservative estimate of the extent of carbonation at
377 Woodsreef.

378 ## Discussion

379 ### Geochemical processes at Woodsreef

There is a distinct difference between the mineralogy of the shallow tailings and carbonate surface crusts found at Woodsreef. The shallow tailings sample, 13WR2-6, was taken from the upper 30 cm of tailings material and did not contain a surface crust. It is notable that it does not contain visible hydromagnesite (observable in hand specimens as a powdery white precipitate and cement) given the widespread formation of surficial, shallow carbonate crusts at Woodsreef. Hydromagnesite is not detectable in XRD patterns collected with either instrument for 13WR2-6, which implies it is either completely absent from the sample or is present below the detection limit of either XRD instrument. Similarly, pyroaurite is barely detectable in sample 13WR2-6. The refined abundances of pyroaurite in the sample were 1.2 wt% (inXitu Terra) and 2.6 wt% (Bruker D8 Advance), near the detection limit of the inXitu Terra and giving absolute errors of comparable magnitude to those determined for the artificial tailings. The refined abundances for pyroaurite may carry large errors based on the analysis of synthetic samples, in spite of this phase being visibly present and detectable in XRD patterns.

Samples that were exposed to the atmosphere, including samples waste rock (13WR1-3) and the crusts on the tailings surface (13WR2-2, 13WR2-5, 13WR2-8), contained carbonate minerals at abundances well above the detection limit of the portable XRD. The refined abundance of hydromagnesite across the different samples varies between 2.5 and 8.8 wt% for the inXitu Terra and 6.7 and 12.5 wt% for the D8 Advance. Absolute error values for hydromagnesite abundances of <5 wt% (as determined from analysis of the artificial tailings) are 0.2−1.0 wt%, which is significantly lower than even the lowest refined abundance for hydromagnesite in these samples. This is a good indication that the refined abundances for hydromagnesite in samples 13WR2-2, 13WR2-5, 13WR2-8 and 13WR1-3 are likely accurate to within the error determined from synthetic mixtures (~25% relative). Furthermore, peaks belonging to hydromagnesite are clearly

403 detectable in the XRD pattern for sample 13WR2-2, as can be seen in Figure 2b. The relative
404 abundance of hydromagnesite in 13WR2-2 and Artrock4 is visually similar (Figure 2b) and
405 Rietveld refinement results for the two samples yield similar abundances of hydromagnesite
406 within error (8.8 wt% and 12.5 wt% respectively using the inXitu Terra). Pyroaurite is present
407 within the crust samples above the detection limits of both instruments, with refined abundances
408 between 1.8 and 13.6 wt%.

409 Importantly, the abundance of hydromagnesite estimated for synthetic tailings that contained >5
410 wt% hydromagnesite (Artock2-4) was underestimated with the magnitude of the estimation
411 increasing with higher abundances of hydromagnesite. Artrock 2 was estimated to contain 4.7 wt%
412 hydromagnesite using inXitu Terra data (known value 5.0 wt%) whereas Artrock4 was estimated
413 to contain 11.1 wt. % using inXitu Terra data (known value 15 wt%). This trend in the synthetic
414 tailings results suggests that refined abundances of hydromagnesite in Woodsreef tailings
415 samples may also be underestimated, reinforcing that any carbon accounting undertaken using
416 this refinement method would represent a conservative estimate of the amount of CO_2 that has
417 been sequestered.

418 Oskierski et al. (2013b) found an average hydromagnesite content of 12.9 wt% and an average
419 pyroaurite content of 5.6 wt% within the vertical surface crusts at Woodsreef. Our refinement
420 results for the abundance of hydromagnesite and pyroaurite are comparable to those reported by
421 Oskierski et al. (2013b) who used the internal standard method (Alexander and Klug, 1948) and
422 the reference intensity ratio method (Chung, 1974) for quantitative phase analysis. This
423 approach can be very accurate; however, it requires calibration, the use of an internal standard,
424 and does not provide simultaneous quantification of all phases.

425 The carbonated crusts on the surface of the tailings pile at Woodsreef have formed by reaction of
426 tailings with carbonic acid that is naturally present in rainwater (Oskierski et al., 2013b). As
427 rainwater permeates through the tailings pile it reacts with serpentine and other gangue minerals
428 such as brucite [$Mg(OH_2)$] to form hydromagnesite and pyroaurite, which consolidate the
429 surrounding tailings into a crust. The formation of sulfate efflorescence crusts has been found to
430 reduce the permeability of tailings crusts in other mine tailings facilities (Acero et al., 2007).
431 Thus, the formation of carbonate crust is likely to act in a similar fashion, progressively
432 preventing ingress of rainwater and dissolved inorganic carbonate deeper into the tailings,
433 leading to the distinct difference observed in the mineralogy of surficial carbonate crusts, and
434 unconsolidated shallow tailings which are less carbonated. Thus, the formation of carbonates in
435 the tailings pile at Woodsreef could be a self-limiting reaction, similar to that described in the
436 tailings storage facility at the Mount Keith Nickel Mine (Wilson et al., 2014).

437 The presence of pyroaurite in the surface crusts, and to a lesser extent the shallow unconsolidated
438 tailings, is an interesting point to consider. Pyroaurite has been previously reported to form from
439 the carbonation of brucite in serpentinites (Mumpton and Thompson, 1966). Brucite was
440 detected at low abundances in several of our tailings samples and has been reported at
441 Woodsreef by previous studies (Oskierski et al., 2013b). This could mean that there are multiple
442 carbonation reaction fronts occurring in the tailings with (1) the formation of hydromagnesite (or
443 other hydrated magnesium carbonate minerals) occurring under ideal geochemical conditions
444 near the surface where a supply of atmospheric CO_2 is available and (2) pyroaurite formation
445 from brucite occurring deeper into the tailings pile where CO_2 is limited and geochemical
446 conditions are less than ideal. This has been shown to occur in laboratory experiments:
447 McCutcheon et al. (2016) demonstrated that pyroaurite forms under CO_2 limited conditions in

448 Woodsreef tailings but that hydrated Mg-carbonates form instead when more CO_2 is supplied by
449 inoculating the tailings with cyanobacteria.

450 Using the refined abundances of hydromagnesite and pyroaurite in the Woodsreef samples it is
451 possible to make an estimate of the amount of CO_2 sequestered in the tailings (Table 2). More
452 robust quantification would require extensive and systematic sampling of the tailings pile to
453 depth (Wilson et al., 2014). There is a significant difference in the amount of CO_2 sequestered in
454 the carbonate crust samples and samples of the shallow unconsolidated tailings present beneath
455 the crusts. The shallow tailings sample 13WR2-6 is estimated to contain between 0.8 and 3.9
456 grams of CO_2 per kilogram of material (according to data from the inXitu Terra and Bruker D8
457 respectively). Contrastingly, values for the crust samples are significantly higher, with estimates
458 of CO_2 sequestered falling between 26.4 and 50.8 g/kg of material. Because hydromagnesite
459 abundance is consistently underestimated in the artificial tailings samples, it is likely these values
460 represent a conservative estimate of the amount of CO_2 sequestered in the tailings at Woodsreef.

461 **Instrument and method comparison**

462 The similarity between (1) our results using Rietveld refinements with a portable and laboratory-
463 based XRD and (2) the results of Oskierski et al. (2013b), which used a different methodology
464 with a laboratory-based XRD, is highly encouraging. We have shown that XRD data from a
465 portable instrument combined with the PONKCS method for mineral quantification produces
466 results with a similar degree of accuracy to laboratory-based instrument data with an internal
467 standard. The average bias value for samples analysed using the inXitu Terra was 8.2 wt%. This
468 compares well with the average bias value of 9.6 wt% obtained using the Bruker D8 Advance
469 and 11.7 wt% which was obtained by Wilson et al. (2009) for similar samples and methods. Our
470 results demonstrate that the PONKCS method can be used to produce accurate quantitative

estimates of mineral abundance and the extent of carbon mineralisation from data collected using a portable XRD.

Implications

Portable XRD instruments represent an important step forward for mineral identification in the field, which has traditionally only been possible through the examination of specimens as hand samples. Applying the PONKCS method to data obtained with a portable instrument such as the inXitu Terra makes it possible to perform quantitative mineralogical analysis of clay-bearing samples in the field using a Rietveld-compatible approach. This combination of instrument and technique eliminates the need to return to the laboratory for results, allowing for the modification of sampling strategies and rapid identification of areas of interest. This could prove invaluable during the initial investigation and monitoring of a field site. By analysing samples in the field and using that information to make informed decisions about where to sample researchers can ensure that there are no knowledge gaps that must be filled during a later excursion. In this way portable XRD instruments have the capacity to become an invaluable tool that can assist and improve monitoring of element cycling, including carbon mineralisation, in natural and industrial landscapes.

Acknowledgements

Funding for this work was provided by grants from Carbon Management Canada and the New South Wales Department of Industry to S.A.W. and G.S. We would like to acknowledge the assistance of Kate Maddison, Nick Staheyeff, Catherine Karpiel and Brad Mullard from the NSW Department of Industry for granting us access to the field site and for their support of our work at Woodsreef. Our particular thanks go to K.M for her knowledgeable advice and support

493 in the field. We would also like to thank Ben Grguric from the South Australian Museum for
494 providing us with samples of iowaite and Marion Anderson of Monash University for providing
495 us with samples of magnetite. We are grateful to Denise Levitan and an anonymous reviewer for
496 their constructive comments, which have improved this manuscript, and to Mickey Gunter for
497 editorial handling.

498 References

499 Acero, P., Ayora, C., and Carrera, J. (2007) Coupled thermal, hydraulic and geochemical evolution of
500 pyritic tailings in unsaturated column experiments. Geochimica et Cosmochimica Acta, 71(22),
501 5325-5338.
502 Alexander, L., and Klug, H.P. (1948) Basic Aspects of X-Ray Absorption in Quantitative Diffraction
503 Analysis of Powder Mixtures. Analytical Chemistry, 20(10), 886-889.
504 Assima, P.G., Larachi, F., Beaudoin, G., Molson, J.W., and (2012) CO2 sequestration in chrysotile
505 mining residues - Implication of watering and passivation under environmental conditions.
506 Industrial & Engineering Chemistry Research.
507 Bea, S.A., Wilson, S.A., Mayer, K.U., Dipple, G.M., Power, I.M., and Gamazo, P. (2012) Reactive
508 transport modeling of natural carbon sequestration in ultramafic mine tailings. Vadose Zone
509 Journal, 11(2).
510 Beinlich, A., and Austrheim, H. (2012) In situ sequestration of atmospheric CO2 at low temperature and
511 surface cracking of serpentinized peridotite in mine shafts. Chemical Geology, 332–333, 32-44.
512 Bish, D.L., Blake, D.F., Vaniman, D.T., Chipera, S.J., Morris, R.V., Ming, D.W., Treiman, A.H., Sarrazin,
513 P., Morrison, S.M., Downs, R.T., Achilles, C.N., Yen, A.S., Bristow, T.F., Crisp, J.A.,
514 Morookian, J.M., Farmer, J.D., Rampe, E.B., Stolper, E.M., Spanovich, N., and Team, M.S.
515 (2013) X-ray Diffraction results from Mars Science Laboratory: Mineralogy of Rocknest at Gale
516 Crater. Science, 341(6153).
517 Bish, D.L., and Howard, S.A. (1988) Quantitative phase analysis using the Rietveld method. Journal of
518 Applied Crystallography, 21(2), 86-91.
519 Blake, D.F., Morris, R.V., Kocurek, G., Morrison, S.M., Downs, R.T., Bish, D., Ming, D.W., Edgett, K.S.,
520 Rubin, D., Goetz, W., Madsen, M.B., Sullivan, R., Gellert, R., Campbell, I., Treiman, A.H.,
521 McLennan, S.M., Yen, A.S., Grotzinger, J., Vaniman, D.T., Chipera, S.J., Achilles, C.N., Rampe,
522 E.B., Sumner, D., Meslin, P.-Y., Maurice, S., Forni, O., Gasnault, O., Fisk, M., Schmidt, M.,
523 Mahaffy, P., Leshin, L.A., Glavin, D., Steele, A., Freissinet, C., Navarro-González, R., Yingst,
524 R.A., Kah, L.C., Bridges, N., Lewis, K.W., Bristow, T.F., Farmer, J.D., Crisp, J.A., Stolper, E.M.,
525 Des Marais, D.J., Sarrazin, P., and Team, M.S. (2013) Curiosity at Gale Crater, Mars:
526 Characterization and Analysis of the Rocknest Sand Shadow. Science, 341(6153).
527 Brindley, G.W. (1945) XLV. The effect of grain or particle Size on x-ray reflections from mixed powders
528 and alloys, considered in relation to the quantitative determination of crystalline substances by x-
529 ray methods. Philosophical Magazine Series 7, 36(256), 347-369.
530 Cheary, R.W., and Coelho, A. (1992) A fundamental parameters approach to X-ray line-profile fitting.
531 Journal of Applied Crystallography, 25(2), 109-121.
532 Chipera, S., and Bish, D. (2002) FULLPAT: A full-pattern quantitative analysis program for X-ray
533 powder diffraction using measured and calculated patterns. Journal of Applied Crystallography,
534 35, 744-749.

Chung, F.H. (1974) Quantitative Interpretation of X-ray Diffraction Patterns of Mixtures. 1. Matrix-Flushing Method for Quantitative Multicomponent Analysis. Journal of Applied Crystallography, 7(6).

Dollase, W. (1986) Correction of intensities for preferred orientation in powder diffractometry: application of the March model. Journal of Applied Crystallography, 19(4), 267-272.

Falini, G., Foresti, E., Gazzano, M., Gualtieri, A.F., Leoni, M., Lesci, I.G., and Roveri, N. (2004) Tubular-shaped stoichiometric chrysotile nanocrystals. Chemistry, 10(12), 3043-9.

Harrison, A.L., Power, I.M., and Dipple, G.M. (2013) Accelerated carbonation of brucite in mine tailings for carbon sequestration. Environmental Science and Technology, Special edition: Carbon Sequestration.

Hill, R.J., and Howard, C.J. (1987) Quantitative phase analysis from neutron powder diffraction data using the Rietveld method. Journal of Applied Crystallography, 20(6), 467-474.

Hitch, M., Ballantyne, S.M., and Hindle, S.R. (2010) Revaluing mine waste rock for carbon capture and storage. International Journal of Mining, Reclamation and Environment, 24(1), 64-79.

IPCC. (2013) Climate Change 2013: The Physical Science Basis. IPCC Working Group 1.

-. (2014) Climate Change 2014 Mitigation of Climate Change. IPCC Working Group 3.

Järvinen, M. (1993) Application of symmetrized harmonics expansion to correction of the preferred orientation effect. Journal of Applied Crystallography, 26(4), 525-531.

Kump, L.R., Brantley, S.L., and Arthur, M.A. (2000) Chemical Weathering, atmospheric CO_2 and climate. Annual Review of Earth and Planetary Sciences, 28, 611-67.

Lackner, K.S. (2002) Carbonate Chemistry for Sequestering Fossil Carbon. Annual Review of Energy and the Environment, 27(1), 193-232.

Lackner, K.S. (2003) A Guide to CO_2 Sequestration. Science, 300, 1677-1678.

Lackner, K.S., Wendt, C.H., Butt, D.P., Joyce Jr, E.L., and Sharp, D.H. (1995) Carbon dioxide disposal in carbonate minerals. Energy, 20(11), 1153-1170.

Laughton, C.A., and Green, N. (2002) Woodsreef Magnesium Project An example of sustainable mineral waste processing from mined ore and its utilisation to produce refined metal products. Green Processing 2002. New South Wales Department of Mineral Resources, St Leonards, N.S.W., Australia, Cairns, QLD.

Lechat, K., Lemieux, J.M., Molson, J.W., Beaudoin, G., and Hebert, R. (2016) Field evidence of CO_2 sequestration by mineral carbonation in ultramafic milling wastes, Thetford Mines, Canada. International Journal of Greenhouse Gas Control, 47, 110-121.

March, A. (1932) Mathematische theorie der regelung nach der korn gestalt bei affiner deformation. Z. Kristallogr. , 81, 285-297.

Matter, J.M., Stute, M., Snæbjörnsdottir, S.Ó., Oelkers, E.H., Gislason, S.R., Aradottir, E.S., Sigfusson, B., Gunnarsson, I., Sigurdardottir, H., Gunnlaugsson, E., Axelsson, G., Alfredsson, H.A., Wolff-Boenisch, D., Mesfin, K., Taya, D.F.d.l.R., Hall, J., Dideriksen, K., and Broecker, W.S. (2016) Rapid carbon mineralization for permanent disposal of anthropogenic carbon dioxide emissions. Science, 352(6291), 1312-1314.

McCutcheon, J., Dipple, G.M., Wilson, S.A., and Southam, G. (2015) Production of magnesium-rich solutions by acid leaching of chrysotile: A precursor to field-scale deployment of microbially enabled carbonate mineral precipitation. Chemical Geology, 413, 119-131.

McCutcheon, J., Wilson, S.A., and Southam, G. (2016) Microbially accelerated carbonate mineral precipitation as a strategy for in situ carbon sequestration and rehabilitation of asbestos mine sites. Environmental Science & Technology, 50(3), 1419-1427.

Mellini, M., and Viti, C. (1994) Crystal structure of lizardite-1T from Elba, Italy. American Mineralogist, 79(11-12), 1194-1198.

Merril, R.J., Butt, B.C., Forrest, V.C., Purdon, G., and Bramley-Moore, R.A. (1980) Asbestos Production at Chrysotile Corporation of Australia Pty. Limited, Barraba, N.S.W. In J.T. Woodcock, Ed. Mining and Metallurgical Practices in Australasia, 10, p. 669-673. The Australasian Institute of

Mining and Metallurgy, Clunies Ross House, 191 Royal Parade, Parkville, Victoria, Australia 3052.

Mumpton, F.A., and Thompson, C.S. (1966) The Stability of Brucite in the Weathering Zone of the New Idria Serpentinite. Clays and Clay Minerals, 14(1), 249-257.

Oelkers, E.H., Gislason, S.R., and Matter, J. (2008) Mineral Carbonation of CO_2. Elements, 4, 333-337.

Omotoso, O., McCarty, D.K., Hillier, S., and Kleeberg, R. (2006) Some Successful Approaches to Qunatitative Mineral Analysis as Revealed by the 3RD Reynolds Cup Contest. Clays and Clay Minerals, 54(6), 748-760.

Oskierski, H.C., Dlugogorski, B.Z., and Jacobsen, G. (2013a) Sequestration of atmospheric CO2 in a weathering-derived, serpentinite-hosted magnesite deposit: 14C tracing of carbon sources and age constraints for a refined genetic model. Geochimica et Cosmochimica Acta, 122(0), 226-246.

Oskierski, H.C., Dlugogorski, B.Z., and Jacobsen, G. (2013b) Sequestration of atmospheric CO_2 in chrysotile mine tailings of the Woodsreef Asbestos Mine, Australia: Quantitative Mineralogy, isotopic fingerprinting and carbonation rates. Chemical Geology.

Pawley, G. (1981) Unit-cell refinement from powder diffraction scans. Journal of Applied Crystallography, 14(6), 357-361.

Power, I.M., McCutcheon, J., Harrison, A.L., Wilson, S.A., Dipple, G.M., Kelly, S., Southam, C., and Southam, G. (2014) Strategizing Carbon-Neutral Mines: A Case for Pilot Projects. Minerals 4, 399-436.

Power, I.M., Wilson, S.A., and Dipple, G.M. (2013) Serpentinite Carbonation for CO_2 Sequestration. Elements, 9, 115-121.

Pronost, J., Beaudoin, G., Lemieux, J.M., Hébert, R., Constantin, M., Marcouiller, S., Klein, M., Duchesne, J., Molson, J.W., Larachi, F., and Maldague, X. (2012) CO_2-depleted warm air venting from chrysotile milling waste (Thetford Mines, Canada): Evidence for in-situ carbon capture from the atmosphere. Geology, 40(3), 275-278.

Rietveld, H. (1969) A profile refinement method for nuclear and magnetic structures. Journal of Applied Crystallography, 2(2), 65-71.

Scarlett, N.V.Y., and Madsen, I.C. (2006) Quantification of phases with partial or no known crystal structures. Powder Diffraction, 21(04), 278-284.

Seifritz, W. (1990) CO_2 disposal by means of silicates Nature, 345.

Taut, T., Kleeberg, R., and Bergmann, J. (1998) The new Seifert Rietveld program BGMN and its application to quantitative phase analysis. Materials Structure, 5(1), 57-66.

Vaniman, D., Bish, D., Blake, D., Elliott, S.T., Sarrazin, P., Collins, S.A., and Chipera, S. (1998) Landed XRD/XRF analysis of prime targets in the search for past or present Martian life. Journal of Geophysical Research: Planets, 103(E13), 31477-31489.

Wilson, S.A., Dipple, G.M., Power, I.M., Thom, J.M., Anderson, R.G., Raudsepp, M., Gabites, J.E., and Southham, G. (2009a) Carbon Dioxide Fixation within Mine Wastes of Ultramafic-Hosted Ore Deposits: Examples from the Clinton Creek and Cassiar Chrysotile Deposits, Canada. Economic geology, 104, 95–112.

Wilson, S.A., Harrison, A.L., Dipple, G.M., Power, I.M., Barker, S.L.L., Mayer, K.U., Fallon, S.J., Raudsepp, M., and Southam, G. (2014) Offsetting of CO_2 emissions by air capture in mine tailings at the Mount Keith Nickel mine, Western Australia: Rates, controls and propects for carbon neutral mining. International Journal of Greenhouse Gas Control, 25, 121-140.

Wilson, S.A., Raudsepp, M., and Dipple, G.M. (2006) Verifying and quantifying carbon fixation in minerals from serpentine-rich mine tailings using the Rietveld method with X-ray powder diffraction data. American Mineralogist, 91(8-9), 1331-1341.

Wilson, S.A., Raudsepp, M., and Dipple, G.M. (2009b) Quantifying carbon fixation in trace minerals from processed kimberlite; a comparative study of quantitative methods using X-ray powder diffraction data with applications to the Diavik diamond mine, Northwest Territories, Canada. Applied Geochemistry, 24(12), 2312-2331.

635

636

637

638

639

640

641

642

643 **Figure Captions**

644 **Figure 1. (a)** Aerial photo of the Woodsreef mine site (courtesy of NSW Department of
645 Industry). **(b)** Location of Woodsreef within Australia. **(c)** Thin horizontal carbonate crust,
646 sample 13WR2-2 (pencil for scale). **(d)** Thick vertical crust, sample 13WR2-5 (hammer for
647 scale). **(e)** Non-carbonated shallow tailings, sample 13WR2-6 (spatula for scale).

648 **Figure 2.** Comparison between inXitu Terra XRD patterns of natural and artificial tailings
649 samples with highest and lowest hydromagnesite abundance **(a)** 13WR2-2 and Artrock4 (highest
650 abundances) and **(b)** 13WR2-6 and Artrock1 (lowest abundances).

651 **Figure 3.** Run time comparison for the inXitu Terra. XRD patterns are for sample Artrock1
652 analysed for 15, 60 and 128 minutes respectively.

653 **Figure 4.** Error values between Rietveld refinement results and known compositions of the
654 artificial tailings samples. Absolute error values are given for refinements of the **(a)** inXitu Terra

655 and **(b)** Bruker D8 data. The corresponding relative errors are plotted in **(c)** for inXitu Terra data

656 and **(d)** for Bruker D8 data.

657

658 **Table 1.** Comparison of known and refined values for the compositions of synthetic tailings

Sample	Abundance	Magnetite + Hematite	Brucite	Pyroaurite + Iowaite	Hydromag-nesite	Chrysotile	Total	R_{wp} [a]	χ^2 [b]	d [c]	Total bias[d]
Artrock1	Weighed (wt%)	7.1	1.0	2.0	1.1	88.8	100.0				
	Terra (wt%)	7.3	0.6	0.5	1.7	89.9	100.0	10.0	1.4	0.3	3.8
	bias abs and rel [e]	+0.2, 2.8	-0.4, 40	-1.5, 75	+0.6, 55	+1.1, 1.2					
	D8 (wt%)	4.4	2.2	1.4	1.5	90.5	100.0	12.9	3.7	0.3	6.6
	bias abs and rel [e]	-2.7, 38	+1.2, 120	-0.6, 30	+0.4, 36	+1.7, 1.9					
Artrock2	Weighed (wt%)	5.0	1.7	3.3	5.0	85.0	100.0				
	Terra (wt%)	6.3	0.2	1.2	4.7	87.7	100.0	9.3	1.2	3.3	7.9
	bias abs and rel [e]	+1.3, 26	-1.5, 88	-2.1, 36	-0.3, 6	+2.7, 3.2					
	D8 (wt%)	2.7	1.1	2.6	4.7	88.9	100.0	11.7	3.5	0.2	7.9
	bias abs and rel [e]	-2.3, 46	-0.6, 35	-0.7, 21	-0.3, 6	+3.9, 4.6					
Artrock3	Weighed (wt%)	5.0	1.7	3.3	10.0	80.0	100.0				
	Terra (wt%)	5.5	0.0	1.6	8.8	84.1	100.0	8.7	1.0	0.5	9.2
	bias abs, %	+0.5, 10	-1.7, 100	-1.7, 52	-1.2, 12	+4.1, 5.1					
	D8 (wt%)	3.5	1.0	2.6	6.7	86.1	100.0	11.4	3.6	0.2	12.3
	bias abs and rel [e]	-1.5, 30	-0.7, 41	-0.7, 21	-3.3, 33	+6.1, 7.7					
Artrock4	Weighed (wt%)	5.0	1.7	3.4	15.0	74.9	100.0				
	Terra (wt%)	7.2	0.7	2.3	11.1	78.7	100.0	8.1	1.0	0.4	12.0
	bias abs and rel [e]	+2.2, 44	-1.0, 59	-1.1, 32	-3.9, 26	+3.8, 5.1					
	D8 (wt%)	3.3	1.5	3.1	11.5	80.6	100.0	12.5	4.0	0.2	11.5
	bias abs and rel [e]	-1.7, 34	-0.2, 12	-0.3, 8.8	-3.5, 23	+5.7, 7.6					

659 [a] Weighted pattern residual, a function of the least-squares residual (%).
660 [b] Reduced chi-squared statistic for the least-squares fit.
661 [c] Weighted Durbin–Watson statistic.
662 [d] Total bias (Δ) = $\sum$ abs($W_{i,\,actual} - W_{i,\,reported}$), W_i is the weight% of the i^{th} mineral. Given in units of wt%.
663 [e] Absolute (wt%) and relative (%) deviation of refined value from weighed mineral abundance.

This is a preprint, the final version is subject to change, of the American Mineralogist (MSA)
Cite as Authors (Year) Title. American Mineralogist, in press.
(DOI will not work until issue is live.) DOI: http://dx.doi.org/10.2138/am-2017-5953

664 **Table 2.** Composition of Woodsreef tailings samples using inXitu Terra and Bruker D8

Sample	**13WR1-3 (vein)**		**13WR2-2 (crust)**		**13WR2-5 (crust)**		**13WR2-6 (tailings)**		**13WR2-8 (crust)**	
Phase	**Terra**	**D8**	**Terra**	**D8**	**Terra**	**D8**	**Terra**	**D8**	**Terra**	**D8**
Pyroaurite	2.9	13.6	2.4	5.0	2.1	2.6	1.2	2.6	1.8	7.3
Magnetite	4.1	1.3	2.5	4.9	3.3	7.4	2.5	5.0	4.2	2.8
Brucite				1.2	0.4	1.3		1.8		2.2
Hydromagnesite	5.3	4.9	8.8	12.5	6.6	10.4			2.2	6.7
Quartz		0.1	0.1	0.2		0.4		0.4		
Forsterite			2.8	2.1		4.4	1.7	4.6		3.3
Enstatite		0.2				1.2	1.3	2.5		0.9
Calcite				0.1		0.4		0.5		0.2
Chrysotile + Lizardite	87.7	80.0	83.4	74.1	87.7	72.0	93.2	82.7	91.8	76.6
Total	100.0	100.0	100.0	100.0	100.0	100.0	100.0	100.0	100.0	100.0
R_{wp}[a]	9.3	11.2	8.7	12.0	8.8	13.2	8.1	16.0	8.8	14.0
χ^{2}[b]	1.2	3.1	1.0	3.2	0.9	3.5	1.0	4.3	1.0	3.7
d[c]	0.3	0.2	0.5	0.2	0.5	0.2	0.5	0.1	0.5	0.2
CO_2 sequestered (g/kg tailings)	21.9	27.5	34.7	50.8	26.2	42.6	0.8	3.9	9.5	30.1

665 [a] Weighted pattern residual, a function of the least-squares residual (%).
666 [b] Reduced chi-squares statistic for the least-squares fit.
667 [c] Weighted Durbin Watson statistic.

This is a preprint, the final version is subject to change, of the American Mineralogist (MSA)
Cite as Authors (Year) Title. American Mineralogist, in press.
(DOI will not work until issue is live.) DOI: http://dx.doi.org/10.2138/am-2017-5953

Figure 1

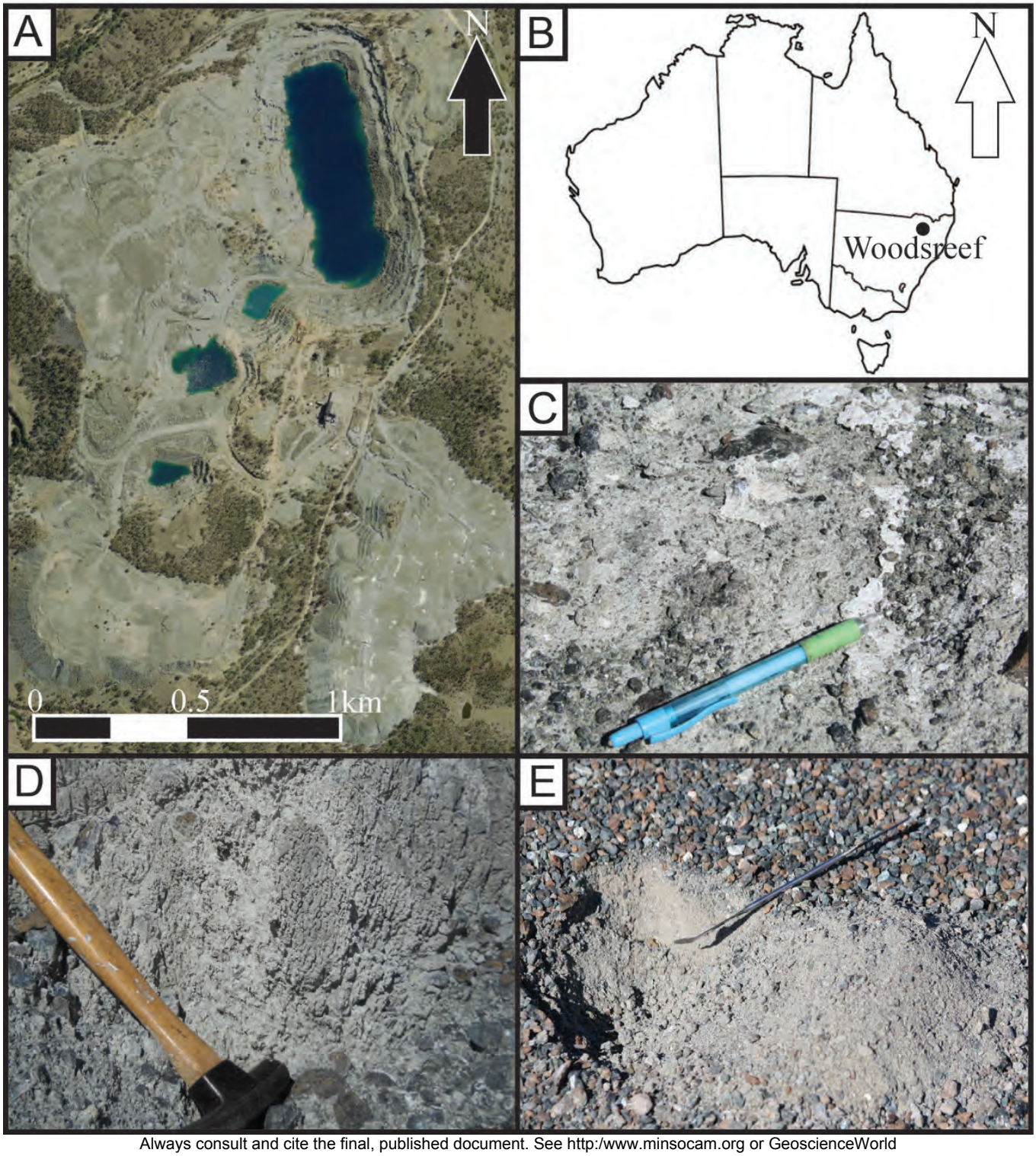

This is a preprint, the final version is subject to change, of the American Mineralogist (MSA)
Cite as Authors (Year) Title. American Mineralogist, in press.
(DOI will not work until issue is live.) DOI: http://dx.doi.org/10.2138/am-2017-5953

Figure 2

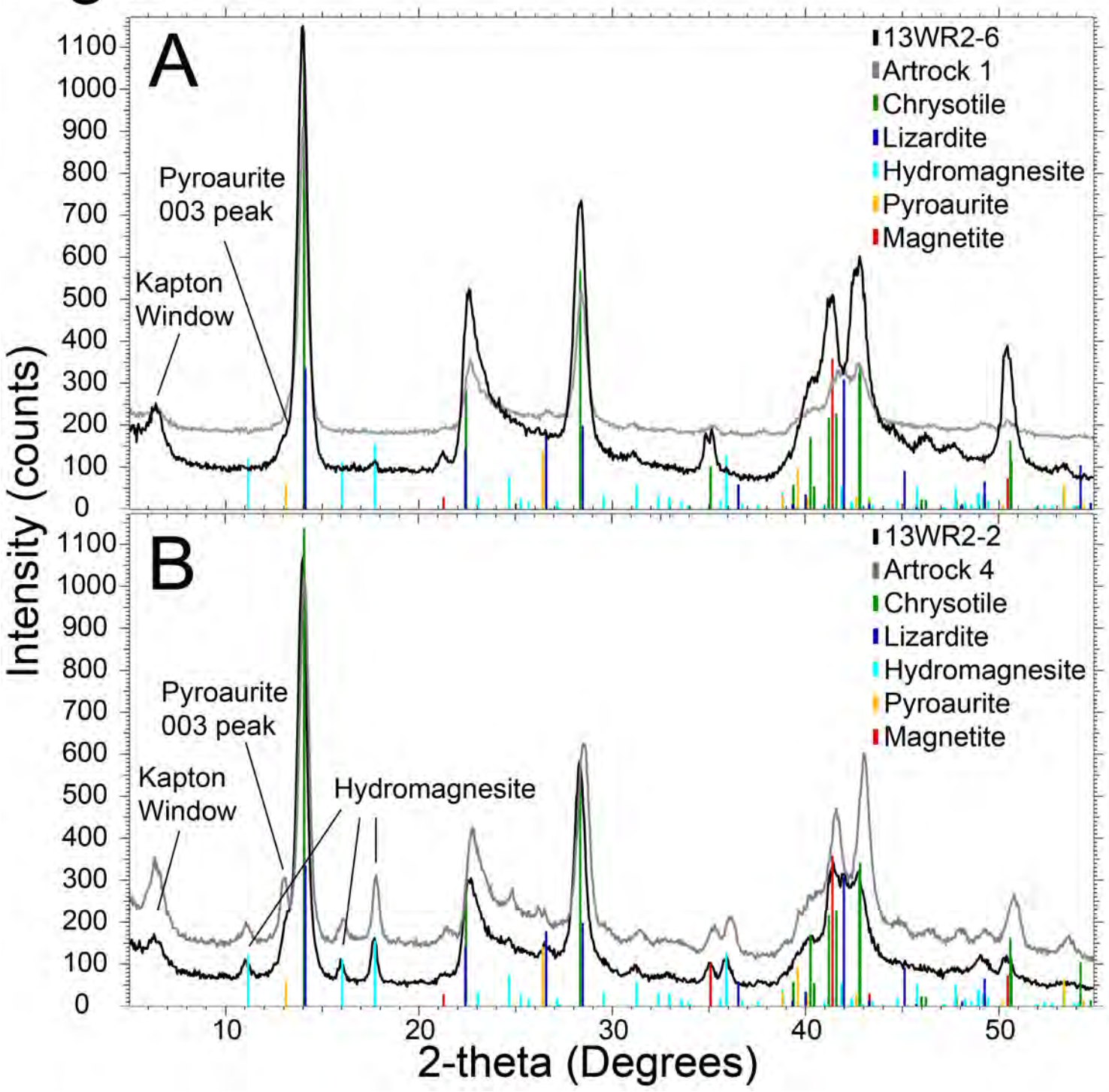

This is a preprint, the final version is subject to change, of the American Mineralogist (MSA)
Cite as Authors (Year) Title. American Mineralogist, in press.
(DOI will not work until issue is live.) DOI: http://dx.doi.org/10.2138/am-2017-5953

Figure 3

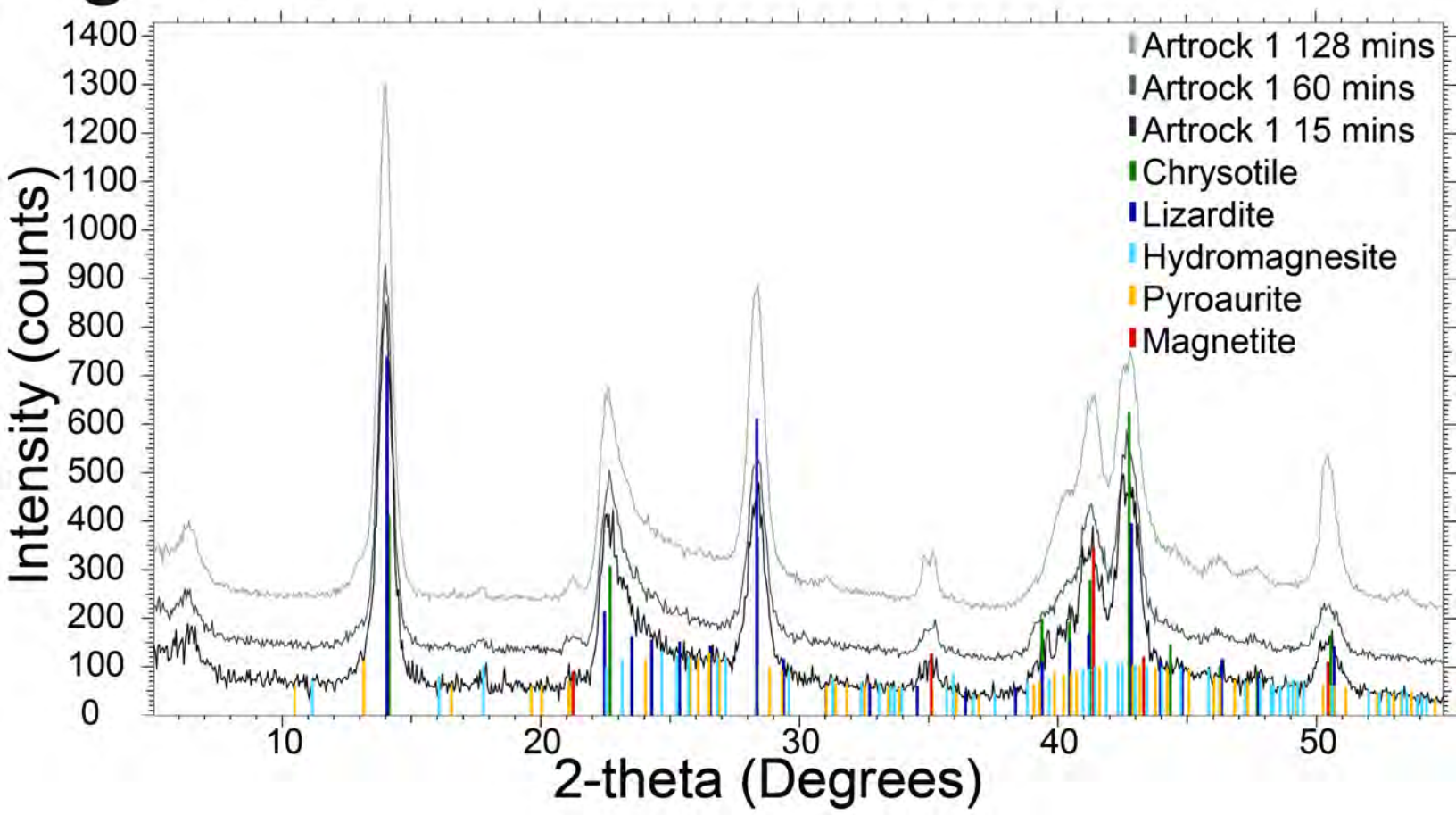

This is a preprint, the final version is subject to change, of the American Mineralogist (MSA)
Cite as Authors (Year) Title. American Mineralogist, in press.
(DOI will not work until issue is live.) DOI: http://dx.doi.org/10.2138/am-2017-5953

Figure 4